EPR and voltammetric evidence for the reversible dimerization of anion radicals of aromatic *meta*-substituted diesters and dithioic *S*,*S*′-diesters

Richard D. Webster

Research School of Chemistry, Australian National University, Canberra ACT 0200, Australia

Received (in Cambridge) 2nd September, Accepted 26th November 1998

The electrochemical behaviour of some alkyl *meta*-substituted (R = Me or Pr) diesters and dithioic *S*,*S*′-diesters of pyridine and benzene (trivial names dipicolinate and isophthalate esters) have been studied by cyclic voltammetry (scan rates = 0.1–50 V s^{-1}) in acetonitrile with 0.1 M tetrabutylammonium hexafluorophosphate as the supporting electrolyte. The cyclic voltammetry data can be interpreted as suggesting that the compounds undergo a one electron reduction to form the corresponding radical anions, which rapidly decompose *via* a chemical step, *i.e.* an EC mechanism, with the chemical step occurring in the order of several milliseconds. However, *in situ* electrochemical-EPR experiments performed during the one electron reduction of the diesters have confirmed the existence of relatively stable radical anions with a much greater lifetime ($t_{1/2}$ > 2–5 s). Furthermore, the very simple nature of the EPR spectra, combined with product analysis data from bulk controlled potential electrolysis experiments, provide very good evidence that the anion radicals are the primary radicals formed by one electron reduction of the starting materials. Therefore, the apparent discrepancy in the lifetimes of the radical anions obtained by voltammetric and spectroscopic methods have been rationalized by considering a reversible dimerization mechanism. Rate constants have been fitted to the cyclic voltammetry data by digital simulation techniques and were estimated to be $k_f \approx 10^3$–10^4 L mol^{-1} s^{-1} (for a radical–radical coupling step) and $k_b \approx 10^{-1}$–10^0 s^{-1} (for the dianion dimer to dissociate to form two anion radicals). Only approximate rate constants could be derived from the experimental curves because a large number of variables needed to be included in the simulations, meaning that no unique combination of variables would give a reasonable data fit. The dimerization reaction is also complicated by a competing reaction where the radical anions or dianions irreversibly decay to form stable products. Thus, the competing decay reaction has also been included in the electrochemical simulations and gives values of $k_d \approx 10^{-1}$–10^0 s^{-1} (assuming a first-order decay).

Introduction

The voltammetric behaviour of all the disubstituted alkyl (alkyl = Pr and some Et and Me) pyridine and benzene esters (**a**) and several of their dithioic *S*,*S*′-diesters (**b**) analogues have recently been reported,[1] as well as the identity and yields of the products obtained by bulk controlled potential electrolysis experiments in acetonitrile.[2] [For brevity the dithioic *S*,*S*′-diesters will be referred to as (S) diesters and the oxygen esters as (O) diesters.]

a **b**

Ar = pyridine or benzene, R = Me, Et or Pr

The (O) and (S) diesters can all be reduced by one electron at negative potentials [−1.61 to −2.69 V *vs.* Fc/Fc^+ (Fc = ferrocene)] with the *para*-substituted (O) and (S) diesters also exhibiting a second reduction step. The stability of the anion radicals formed during the first (least negative) reduction step and the electrochemical reversibility of the reduction process, as measured by cyclic and linear sweep voltammetry, varied considerably between the compounds.[1] On the long time scale, bulk controlled potential electrolysis experiments have shown that most of the (O) ester anion radicals decay *via* a simple bond cleavage mechanism to form the carboxylate anions in very high yield (70–100%), whilst the (S) ester radicals decay *via* a very complicated mechanism often involving aromatic substitution reactions.[2] Using cyclic voltammetry, many of the compounds were shown to display chemically (and electrochemically) reversible behaviour at slow scan rates (v = 100 mV s^{-1}), in the sense that the i_p^{ox}/i_p^{red} ratios were close to one, indicating that the anion radicals formed were stable for at least several seconds, and their existence was confirmed by EPR[1] and UV–VIS spectroscopy.[3] In contrast, other compounds, including the *meta*-substituted (O) and (S) diesters (**1** and **2**), *appeared* to show chemically irreversible behaviour at slow scan rates suggesting that the associated anion radicals of these compounds were much less stable and quickly decompose to form other products.

1 **2**

1a Y = O, R = Me, dimethyl benzene-1,3-dicarboxylate
1b Y = S, R = Pr, *S*,*S*′-dipropyl benzene-1,3-dicarbothioate
2a1 Y = O, R = Me, dimethyl pyridine-2,6-dicarboxylate
2a2 Y = O, R = Pr, dipropyl pyridine-2,6-dicarboxylate
2b Y = S, R = Pr, *S*,*S*′-dipropyl pyridine-2,6-dicarbothioate

In this paper, cyclic voltammetric data that has been obtained at various concentrations and scan rates (0.1–50 V s^{-1}) from several *meta*-disubstituted (O) and (S) diesters of pyridine and benzene are discussed. EPR spectroscopy has shown that the anion radicals of the *meta*-disubstituted (O) and (S) diesters formed by one electron reduction of the parent compounds are surprisingly stable, which has prompted the analysis of the cyclic voltammetry data in terms of a reversible dimerization mechanism.

There has been a steadily growing number of reports of organic anionic, cationic and neutral radical species formed by electrochemical methods being able to undergo reversible dimerization reactions. One of the early reported cases of electrochemically generated anions undergoing reversible dimerization that also created considerable debate in the literature, was the reduction of 9-substituted anthracenes.[4–7] Hammerich and Parker[5] reported that the electrochemical data (cyclic and linear sweep voltammetry) was not supportive of a simple radical–radical dimerization reaction for 9-substituted anthracene radical anions, and suggested that the dimerization proceeded through a π-bonded intermediate dimer dianion as well as through a σ-bonded dimer, in addition to other unidentified steps. In contrast, Amatore *et al.*[6] suggested that 9-substituted anthracene ions were good candidates for a simple radical–radical coupling mechanism, and electrochemical data contrary to that were a result of artefacts in the treatment of the kinetic data. The role of water in the reaction was also disputed between the groups.[5c,6b] An important factor in the identification of the dimerization mechanism was that stable neutral dimers could be isolated in very high yields if the post-electrolysis extraction/protonation procedures were performed in an inert atmosphere,[7b] indicating that the dimerization mechanism definitely occurred through σ-bonded species. Acridine, a nitrogen containing analogue of anthracene, was also found to undergo reversible dimerization following reduction in supercritical ammonia.[8]

Phenoxyl radicals are formed by oxidation of phenolates, with one of the decomposition mechanisms being the formation of dimers.[9] 2,4,6-Trisubstituted-phenoxyls with bulky substituents in the 2- and 6-positions have been found to undergo a range of reversible dimerization, irreversible dimerization or disproportionations depending on the substituent in the 4-position.[10] A key feature in the assignment of the reversible dimerization of the phenolates is that during cyclic voltammetry experiments at faster scan rates the reverse cathodic peak of the oxidation process becomes smaller (due to a large k_f for the dimerization reaction and a relatively small k_b for the reverse monomerization reaction), rather than larger as is the case for irreversible dimerization reactions.[10b]

There have been several recent reports on the ions formed by the oxidation of precursors of conducting polymers undergoing reversible dimerization reactions.[11–14] Cyclic voltammetry studies on the oxidation of diphenylpolyenes[11a] and 3,3′,5,5′-tetramethyl-2,2′-bithiophene[11b] has led to the conclusion that a rapid reversible dimerization occurs between the cation radicals, and that the reversible dimerization can be considered as an alternative mechanism to the bipolaron model for the stabilization of conducting polymers. Semi-empirical molecular calculations have suggested that the dimerization of the diphenylpolyenes and bithiophenes occurs through intermolecularly σ-bonded cations.[11] (The accuracy of molecular orbital calculations in predicting the structure of radical cation intermediates have, however, been questioned.[15])

The reduction of the methyl viologen dication to its cation radical has been studied extensively with voltammetry and spectroscopy with the general consensus being that a π-bonded dimer is reversibly formed.[14,16] Other organic systems that have been identified as undergoing reversible dimerization that have been studied by electrochemical techniques include the anion radicals of ethyl cinnamate,[17] diethyl fumarate,[17b,18] and di- and tricyanobenzenes;[19] and the cation radicals of 2,5-diaryl-1,4-dithiins[20] and the oxidation products of the dianion of bidurenol[21] and the Bu^{t}C$_{60}$ anion.[22]

Experimental

Chemicals and reagents

The (O) diesters were prepared either by refluxing the carboxylic acid in thionyl chloride to make the acid chloride and then in the corresponding alcohol to make the ester or by refluxing the carboxylic acid directly in alcohol with concentrated sulfuric acid.[2] Dimethyl benzene-1,3-dicarboxylate (97%) was purchased from Aldrich. The (S) diesters were prepared by refluxing the aromatic acid chloride in dichloromethane with the correct molar equivalent of propanethiol.[2,23] All solids were recrystallized from either methanol, methanol–water or diethyl ether–petroleum spirits (bp 60–90 °C). Oils were purified by radial chromatography on silica gel with diethyl ether–petroleum spirits (bp 60–90 °C) (3:17) as the eluent. Purity of the compounds was confirmed by NMR, mass spectrometry, TLC and melting points for the solids. High purity acetonitrile (Fisher) was dried immediately prior to use by passing through a column of activated neutral alumina.[24] Tetrabutylammonium hexafluorophosphate (Bu$^n_4$NPF$_6$) from Fluka (puriss, electrochemical grade) was used as received.

Cyclic voltammetry

Cyclic voltammetric experiments were conducted on a 1 mm diameter glassy carbon working electrode using an Eco Chemie Autolab potentiostat 20. An Ag/Ag$^+$ (0.05 M $AgNO_3$ and 0.1 M Bu$^n_4$NPF$_6$ in acetonitrile) reference electrode and a platinum basket auxiliary electrode were used. Test solutions thermostatted to 20 ± 0.2 °C were thoroughly deoxygenated with argon prior to analysis and a continuous stream of argon was passed over the solution when measurements were being performed. Accurate $E^r_{\frac{1}{2}}$-values (reversible half wave potentials) for the compounds under study have been reported previously relative to the ferrocene/ferrocinium redox couple.[1] The experiments were performed by recording cyclic voltammograms in the presence and absence of substrate. The background-subtracted curves were compared with cyclic voltammetry curves simulated using DigiSim 2.1[25] and ESP version 2.4,[26] with the following standard parameters; resistance = 600 ohms, capacitance = 1×10^{-8} F, and transfer coefficients (α) = 0.5.

EPR spectroscopy

First derivative X-band EPR spectra were recorded on either a Bruker ECS-106 spectrometer fitted with a frequency counter or on a Bruker ER 200D spectrometer, both employing a rectangular TE$_{102}$ cavity. In all cases the modulation amplitude was 0.02 mT and the modulation frequency 50–100 kHz. A silica channel electrode using a square of 4 mm × 4 mm gold foil (Goodfellow, 99.95%, 0.25 μm thickness) as the working electrode was used to generate the radical anions *in situ* in the EPR cavity.[27] The solutions were deoxygenated with solvent saturated argon prior to and during the voltammetric experiments and the degassed solutions were flowed through the EPR cavity. The reference electrode was a silver wire situated upstream and the auxiliary electrode a platinum basket situated downstream and well outside the EPR cavity to ensure that there was no interference from any paramagnetic species produced at the auxiliary electrode. The reduction potential was set by first recording a steady state voltammogram and then setting the potential at the top of the limiting current plateaux. Isotropic EPR simulations were performed using the Bruker computer software, WINEPR SimFonia. For all EPR simulations a 100% Lorentzian line shape was calculated and the linewidths listed are given as peak to peak (ΔH_{pp}).

Results and discussion

Cyclic voltammetry

Fig. 1 shows cyclic voltammograms of 2.78 mM dimethyl benzene-1,3-dicarboxylate (**1a**) recorded at several scan rates at a 1 mm diameter glassy carbon electrode in acetonitrile. The solid lines in Fig. 1 are the experimental voltammograms and

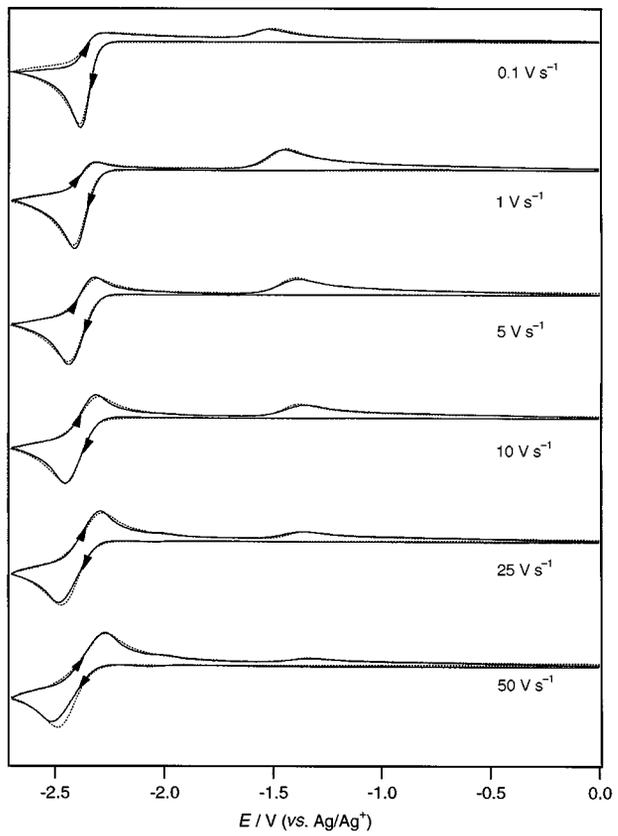

Fig. 1 Cyclic voltammograms of 2.78 mM dimethyl benzene-1,3-dicarboxylate (**1a**) obtained at a GC electrode at a variety of scan rates at 20 °C. Solid line (——) = experimental data, dashed line (---) = simulations. See Table 1 for simulation parameters.

the dashed lines are the simulated voltammograms. A glassy carbon electrode was chosen because it was found that at this surface (as opposed to metal electrodes such as Ag, Au, Hg and Pt) the voltammetry suffers the least interferences from adsorption processes.[2a] When the potential was scanned in the negative direction, a reduction process occurred at *ca.* 2.3–2.5 V with a corresponding one electron cathodic current (i_p^{red}). Switching the potential sweep direction just past the reduction process (−2.7 V) to the positive direction resulted in a very small anodic current (i_p^{ox}) at slow scan rates ($v < 1$ V s^{-1}). Increasing the scan rate from 0.1 V s^{-1} to 50 V s^{-1} resulted in an increase in the i_p^{ox}/i_p^{red} ratio (Fig. 1). Previously, the voltammetric behaviour for this compound[1,2b] was interpreted in terms of an EC (electron transfer followed by a chemical step) mechanism where the reduced species was presumed to be chemically unstable and it was reasoned that fast scan rates were necessary to obtain i_p^{ox}/i_p^{red} ratios approaching 1.[28] However, in light of voltammetric concentration dependence data and EPR evidence (see discussion below) the data have now been analysed according to a reversible dimerization mechanism.

The proposed mechanism for the reduction of **1a** is shown in Scheme 1 with the first step being the one electron reduction of the parent compound to form the radical anion (E mechanism) [Scheme 1, step (1)]. The next step(s) can either occur through a C mechanism [Scheme 1, step (2)] or by a CE mechanism [Scheme 1, steps (3) and (4)]. Overall, steps (1) (occurring twice) and (2) are an EC_{dim} (radical–radical coupling) mechanism, and steps (1), (3) and (4) are an ECE (radical–substrate coupling) mechanism.[15]

The dimer species (A_2^{2-}) can be detected voltammetrically as an oxidation peak present in cyclic voltammograms at *ca.* −1.35 ± 0.15 V (Fig. 1). If the dimer dianion (A_2^{2-}) or radical anion ($A^{\bullet -}$) were 100% stable on the time-scale of the voltammetric experiments illustrated in Fig. 1, then it would be

$A + e^- \rightleftharpoons A^{\bullet -}$	$k_{e(monomer)}$	heterogeneous	(1)
$2A^{\bullet -} \rightleftharpoons A_2^{2-}$	k_f, k_b	homogeneous	(2)
$A^{\bullet -} + A \rightleftharpoons A_2^{\bullet -}$		homogeneous	(3)
$A_2^{\bullet -} + e^- \rightleftharpoons A_2^{2-}$	$k_{e(dimer)}$	heterogeneous	(4)
$A^{\bullet -} \rightleftharpoons B$	k_d	homogeneous	(5)
$A_2^{2-} \rightleftharpoons 2B$		homogeneous	(6)
$A_2^{\bullet -} \rightleftharpoons C + e^-$	$k_{e(dimer)}$	heterogeneous	(7)

Scheme 1 A = starting material, $A^{\bullet -}$ = primary anion radical, A_2^{2-} = dianion dimer, $A_2^{\bullet -}$ = radical dimer, C = oxidation product of $A_2^{\bullet -}$ (which may simply be 2A), and B represents the final products of the reaction, which for the (O) diesters are the carboxylate anions (most probably *via* loss of an alkyl radical) and for the (S) diesters are generally complicated products.[2]

expected that the peak current associated with oxidation of the dimer should decrease as the scan rate is increased, due to less dimer being produced as the dimerization reaction is outrun. However, comparing the voltammograms obtained at 0.1 and 1 V s^{-1} (Fig. 1) shows that the peak current for the oxidation of A_2^{2-} at the slower scan rate (0.1 V s^{-1}) is less than at 1 V s^{-1}. This is most likely due to A_2^{2-} or $A^{\bullet -}$ being chemically unstable and irreversibly decaying in the time taken to scan from −2.7 to −1.35 V. At scan rates faster than *ca.* 1 V s^{-1} the decay reaction is outrun and hence the peak current associated with the oxidation of the dimer decreases with increasing scan rate. Therefore, in order to account for the low concentrations of dimer at slow scan rates ($v < 1$ V s^{-1}), steps (5) and (6) have been included in Scheme 1 for the decay of $A^{\bullet -}$ or A_2^{2-} respectively. Scheme 1, step (7) and the back reaction of step (4) are the oxidation processes for the dimer, and are illustrated as two one electron steps. The oxidation process for the dimer remained chemically irreversible up to the maximum scan rate examined of 50 V s^{-1} (no reduction current was detected when the potential scan direction was reversed just past the oxidation peak for the dimer).

Qualitatively, it was observed that increasing the concentration of **1a** (at a fixed scan rate) resulted in the voltammetric peak current for the oxidation of A_2^{2-} also increasing, whilst decreasing the concentration of **1a** (a fixed scan rate) resulted in the i_p^{ox}/i_p^{red} ratio for the $A^{\bullet -}$/A redox couple increasing. Both of these observations are consistent with a dimerization mechanism, where at high concentrations the dimer dianion is favoured and at low concentrations the equilibrium lies more toward the monomer anion radical.

The dimerization reaction was examined quantitatively by fitting simulated voltammograms to the experimental data between 1–10 mM and scan rates between 0.1–50 V s^{-1}. The simulated voltammograms to the 2.78 mM cyclic voltammetry data for compound **1a** are shown in Fig. 1 and the approximate rate constants for the forward (dimerization, k_f), back (monomerization, k_b) and decay (k_d) reactions are presented in Table 1 along with the relevant heterogeneous electron transfer rates ($k_{e(monomer)}$ and $k_{e(dimer)}$). The deviations of the theoretical voltammograms from the experimental data is partly due to a combination of uncertainty in the exact mechanism (see discussion further below) and experimental difficulties. The anion radicals are extremely oxygen and moisture sensitive and a decrease in the i_p^{ox}/i_p^{red} ratios was observed unless the upmost care was taken in drying and deoxygenating the solvent. (This is due to an ester hydrolysis type reaction,[2b] and not due to an association reaction with water[5c] or changes in solvation effecting the equilibrium,[6b] as have been proposed for 9-substituted anthracene radicals at high concentrations of water.) The error associated with this was the most severe at low substrate concentrations where the ratio of analyte to trace water

Table 1 Rate constants obtained by digital simulation of CV data for an EC_{dim} reversible dimerization mechanism. CV data recorded in acetonitrile (with 0.1 M $Bu^n_4NPF_6$) at a 1 mm diameter GC electrode for concentrations of analytes between 0.5–10 mM and scan rates between 0.1–50 V s^{-1}. $T = 20 \pm 0.2$ °C

Compound	$D_{(monomer)}$ [a]/ $cm^2\ s^{-1}$ ($\pm 2 \times 10^{-6}$)	$D_{(dimer)}$/ $cm^2\ s^{-1}$ ($\pm 4 \times 10^{-6}$)	$E^r_{1/2(monomer)}$/ V [b] (± 0.005)	$E^r_{1/2(dimer)}$ [c]/ V (± 0.1)	$k_{e(monomer)}$ [d]/ $cm\ s^{-1}$	$k_{e(dimer)}$ [d,e]/ $cm\ s^{-1}$	K_{eq} [d]/ $L\ mol^{-1}$	k_f [d]/L $mol^{-1}\ s^{-1}$	k_b [d]/s^{-1}	k_d [d]/s^{-1}
1a	2.0×10^{-5}	1.2×10^{-5}	−2.370	−1.6, −1.7	$1–5 \times 10^{-2}$	$1–5 \times 10^{-3}$	$\sim 10^4–10^5$	$\sim 10^3–10^4$	$10^{-1}–10^0$	$10^{-1}–10^0$
1b	1.5×10^{-5}	9.0×10^{-6}	−2.035	−1.2, −1.3	$1–5 \times 10^{-2}$	$1–5 \times 10^{-3}$	$\sim 10^4–10^5$	$\sim 10^3–10^4$	$10^{-1}–10^0$	$10^{-1}–10^0$
2a1	1.5×10^{-5}	1.0×10^{-5}	−2.170	−1.4, −1.5	$1–5 \times 10^{-2}$	$1–5 \times 10^{-3}$	$\sim 10^4–10^5$	$\sim 10^3–10^4$	$10^{-1}–10^0$	$10^{-1}–10^0$
2a2	1.2×10^{-5}	8.0×10^{-6}	−2.190	−1.4, −1.5	$1–5 \times 10^{-2}$	$1–5 \times 10^{-3}$	$\sim 10^4–10^5$	$\sim 10^3–10^4$	$10^{-1}–10^0$	$10^{-1}–10^0$
2b	1.5×10^{-5}	1.0×10^{-5}	−1.900	−1.3, −1.4	$1–5 \times 10^{-2}$	$1–5 \times 10^{-3}$	$\sim 10^4–10^5$	$\sim 10^3–10^4$	$10^{-1}–10^0$	$10^{-1}–10^0$

[a] Obtained from microelectrode experiments using the relationship $i_d = 4nFaDc$ (where i_d is the limiting current, n is the number of electrons transferred, F is the Faraday constant, a is the radius of the electrode, D is the diffusion coefficient and c is the concentration of analyte) and further refined by digital simulation. [b] Potential *vs.* Ag/Ag^+ (0.05 M $AgNO_3$ in acetonitrile). [c] Potentials for two separate one electron oxidation processes [steps (4) and (7) respectively, Scheme 1]. [d] Approximate homogeneous or heterogeneous rate constants. The large range in these values reflects the high error associated with the simulations due to the high number of variables (see text). [e] Rate constant for two (assumed equivalent) one electron heterogeneous charge transfer processes [steps (4) and (7), Scheme 1].

(and oxygen) was the lowest. Detailed analysis of the responses obtained during CV experiments indicated that adsorption of the compounds occurred and that this was highly electrode dependent.[1,2a] Adsorption often took the form of an increasing baseline (where there would normally be almost zero faradaic current in the absence of adsorption effects) prior to the first reduction process, which became more pronounced at higher concentrations of analyte or if repeated cyclic voltammograms were performed, and resulted in errors in theoretically matching the experimental data (particularly for compounds **2a1** and **2a2**). In some instances the experimental data showed a larger than predicted current at potentials negative of the first reduction step, which is partly caused by background faradaic processes due to the closeness of the reduction process to the solvent/electrolyte breakdown limit, but also due to reduction processes associated with the esters that occur at more negative potentials.[1–3]

There are several uncertainties regarding the exact pathway the reaction follows which resulted in the following mechanistic assumptions being made. (i) The decay reaction was assumed to proceed irreversibly through $A^{\bullet -}$ rather than A_2^{2-} [*i.e.* Scheme 1, step (5) rather than step (6)]. Synthetic scale bulk controlled potential electrolysis experiments have shown that the final products of the one electron reduction of the (O) diesters are the carboxylate anions in high yield (70–100%) (Scheme 2).[2]

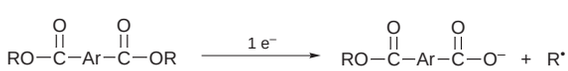

Scheme 2

The ^1H NMR spectra for the electrolyte–product mixture recorded at the completion of the electrolysis were clean in the aromatic region which suggested that only one product was formed, *i.e.* the carboxylate anion, and no evidence was obtained for a dimer type species as a final reaction product.[2] Therefore, the assumption that the decay reaction proceeds through $A^{\bullet -}$ is reasonable. (Note that the alkyl radical, $R^{\bullet}$, in Scheme 2 is a postulated intermediate whose existence has been proposed based on the high yield of the carboxylate anion and the number of electrons transferred in the reaction.[1–3,29]) (ii) The diffusion coefficient (D) of $A^{\bullet -}$ was set to be the same as that of A and the diffusion coefficient of A_2^{2-} was approximated to be $\frac{2}{3}$ that of A. Calculations based on molecular size considerations predict the diffusion coefficients of dimers to be $\frac{2}{3}$ that of their corresponding monomers,[30] while charged species often have similar or slightly smaller D-values than their corresponding neutral entities.[31] (iii) In order to account for the rounded voltammetric peak shape associated with the oxidation of A_2^{2-}, two relatively slow one electron heterogeneous charge transfer processes ($k_{e(dimer)}$ in Table 1) with different oxidation potentials were included in the simulations [Scheme 1, step (7) and the reverse of step (4)]. The slow heterogeneous rate constants also accounted for the large shift in oxidation potential of the dimer to more positive potentials with increasing scan rate (Fig. 1). Finite heterogeneous rate constants were included for the initial one electron reduction of the esters, which were important in improving the match between the theoretical and experimental curves at scan rates >10 V s^{-1}. (vi) Due to the relatively large number of uncertainties in the mechanistic pathway it is difficult to determine absolutely whether the reaction proceeds through an EC_{dim} or ECE mechanism. However, the primary purpose of the simulations was to test the feasibility of the reversible dimerization mechanism, hence the simulations were performed for the simpler EC_{dim} mechanism, similar to Smie and Heinze.[11a]

Similar voltammetric experiments and simulations that were performed on **1a** were also performed on compounds **1b**, **2a1**, **2a2** and **2b** (Table 1). Figs. 2(a) and 2(b) show the cyclic voltammograms (solid line) and corresponding simulations (dashed lines) obtained at a scan rate of 1 V s^{-1} for compounds **1b**, **2a1**, **2a2** and **2b** (at two concentrations) which have been simulated using the same approximations applied to **1a** and the mechanism depicted in Scheme 1. The general features were the same for all of the compounds with the dimer dianions undergoing two relatively slow one electron heterogeneous charge transfer oxidation processes and the voltammetric wave for the oxidation of the dimer going through a maximum in peak current at a scan rate of *ca.* 1 V s^{-1}.

It is apparent from the large number of variables presented in Table 1 that there will not necessarily be a unique combination of kinetic values that will give a reasonable data fit. The uncertainty in the exact mechanistic pathway combined with the experimental difficulties also contributed to the large error associated with the kinetic data. The kinetic values given in Table 1 represent the range over which the rate constants can be expected to be varied and still obtain a reasonable data fit. The simulated data shown in Figs. 1 and 2 were obtained by fitting rate constants which lie within the individual ranges shown in Table 1. If it is considered that the kinetic data obtained from the simulations could vary by as much as a factor of five, then the individual rate constants obtained for compounds **1a**–**2b** can be regarded as equivalent within experimental error. However, despite the large error, the theoretical kinetic values were still extremely important in confirming the dimerization mechanism when compared with the EPR spectroscopic data.

An interesting feature of the cyclic voltammograms shown in Figs. 1 and 2 is that the reverse oxidative peak current (i_p^{ox}) of the reduction process does not become smaller at faster scan rates, as the cathodic peak current (i_p^{red}) does in the analogous

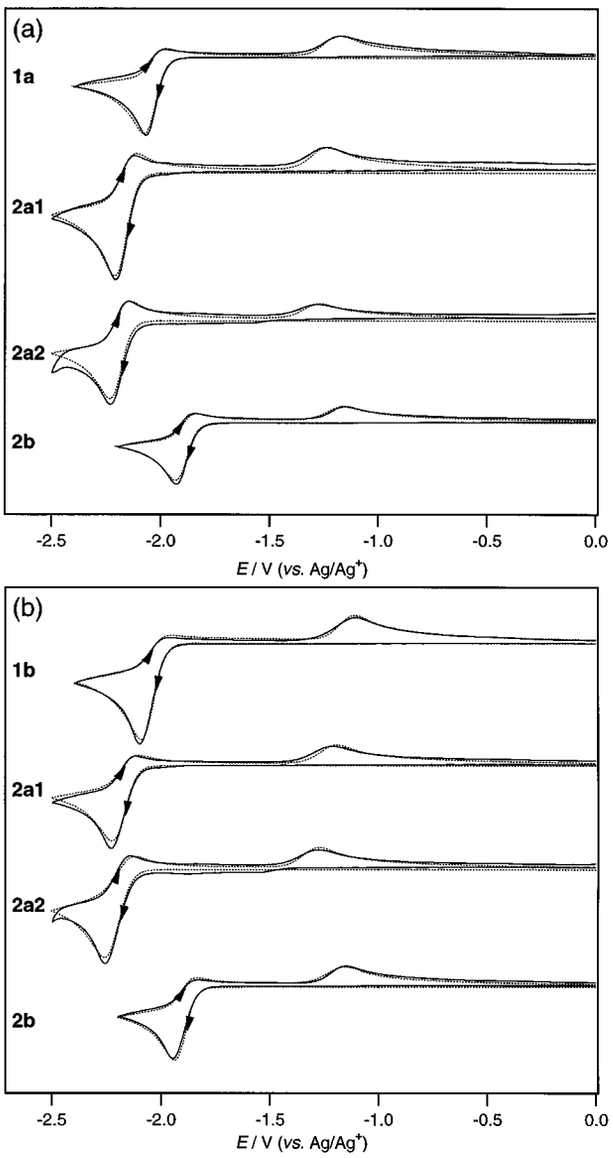

Fig. 2 Cyclic voltammograms recorded at 1 V s^{-1} at a GC electrode at 20 °C. Solid line (——) = experimental data, dashed line (---) = simulations. See Table 1 for simulation parameters. Concentrations are (a) **1b** = 2.12 mM, **2a1** = 2.92 mM, **2a2** = 2.61 mM, **2b** = 1.62 mM (b) **1b** = 7.06 mM, **2a1** = 5.85 mM, **2a2** = 8.69 mM, **2b** = 5.41 mM.

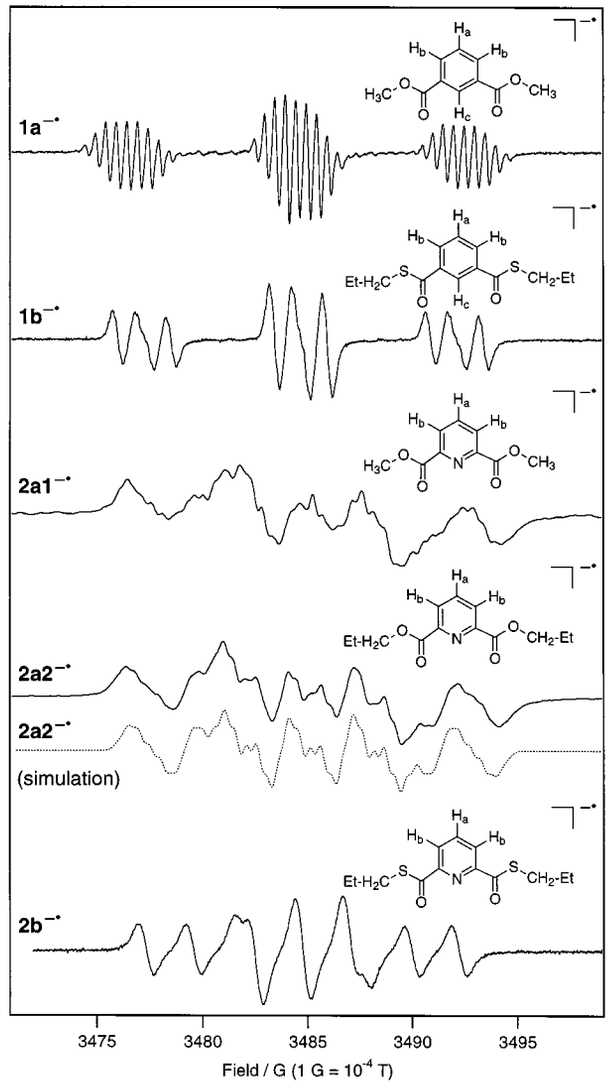

Fig. 3 First derivative EPR spectra of the radical anions obtained in an *in situ* channel electrode flow cell with a 0.4 × 0.4 cm gold foil electrode and with the potential held in the limiting current region for the one electron reduction of the parent molecule. In all cases the modulation amplitude was 0.02 mT, the sweep time 100 s and the time constant 5 ms, except for compounds **2a1**$^{\bullet -}$ and **2a2**$^{\bullet -}$ where the time constant was 1 s. The concentrations were between 0.5–1.0 mM parent compound. **2a2**$^{\bullet -}$ (simulation) is the simulated spectrum of **2a2**$^{\bullet -}$ with $a_N = 0.304$ mT, $a_{H_a} = 0.10$ mT, $a_{H_b} = 0.46$ mT, $a_{CH_2} = 0.045$ mT and $\Delta H_{pp} = 0.053$ mT. Other hyperfine coupling constants are given in Table 2.

oxidative-reversible dimerization of phenolates[10b] or diphenylpolyenes[11a] (see Introduction). The absence of the decrease in i_p^{ox} with increasing scan rate led to the difficulty in initially characterizing this system[1,2] (and perhaps others of this type) and emphasizes the importance that spectroscopy has in characterizing complex electrochemical reactions[32] (see discussion on EPR data below).

EPR spectroscopy

In situ EPR spectra were recorded during the one electron reduction of the compounds in a silica channel electrode with the reduction potential held at the top of the steady state limiting current wave (see Experimental section) and the spectra are shown in Fig. 3. The hyperfine splitting constants of the anion radicals were calculated by simulation of the experimental spectra and are given in Table 2. The spectra for **1a**$^{\bullet -}$ and **1b**$^{\bullet -}$ are similar to those reported by Hirayama[33] and Voss *et al.*[34] respectively.

Estimates on the lifetimes of the anion radicals were also made using the channel electrode arrangement. It has been demonstrated[27] that for a stable electrogenerated radical, *i.e.* a radical that does not decompose before it has flowed out of the spectrometer cavity, relationship (1) holds, where S is

$$(S/i_d) \propto V_f^{2/3} \quad (1)$$

the intensity of the EPR signal, i_d is the limiting Faradic current obtained from the sigmoidal shaped voltammogram and V_f is the volume solution flow rate ($cm^3\ s^{-1}$). Specifically, a plot of lg (S/i_d) *vs.* lg V_f should be a straight line with a slope of $-\frac{2}{3}$. For a radical that is unstable over the course of the experiment this plot will diverge from the ideal slope of $-\frac{2}{3}$, especially at slow flow rates. The data for all the compounds gave straight line log plots with slopes close to $-\frac{2}{3}$ indicating that the anion radicals are stable on the time-scale of the experiments, which allowed a minimum estimate of the lifetime of the radical anions of *ca.* 2–5 s. Previous EPR measurements of the lifetimes of radicals **1b**$^{\bullet -}$ and **2b**$^{\bullet -}$ using an *in situ* stationary solution electrochemical-EPR cell allowed the estimate of the

Table 2 EPR spectroscopic data of radical anions obtained at 20 ± 2 °C in acetonitrile with 0.1 M $Bu^n_4NPF_6$

Compound	Hyperfine coupling constant/mT[a]				
	H_a	H_b	H_c or N	CH_2 or CH_3	ΔH_{pp}
1a$^{\bullet -}$	0.152	0.805	0.058	0.045	0.020
1b$^{\bullet -}$	0.152	0.744	0.100	0.025	0.027
2a1$^{\bullet -}$[b]	0.110	0.465	0.305	0.045	0.060
2a2$^{\bullet -}$[b]	0.110	0.465	0.305	0.045	0.060
2b$^{\bullet -}$	0.050	0.520	0.226	0.025	0.030

[a] Hyperfine coupling constants and peak to peak linewidths were obtained by simulation of the experimental spectra shown in Fig. 3. [b] Due to the anisotropy in the spectra, the hyperfine coupling constants for **2a1**$^{\bullet -}$ and **2a2**$^{\bullet -}$ have an estimated error of 0.01 mT. See Fig. 3 for an example simulation of **2a2**$^{\bullet -}$.

$t_{1/2}$-values of 10 s[2a] and 17 s[2b] respectively. Therefore, the moderately high stability of the radical anions combined with the concentration dependence on the i_p^{ox}/i_p^{red} ratios indicate that a simple EC mechanism (electron transfer followed by rapid irreversible reaction) is unlikely to occur, whereas the reversible dimerization reaction can adequately account for the experimental data.

On first appraisal, the k_f values for the dimerization reaction appear very high and the equilibrium much in favour of the dimer. However, if one considers that the dimerization reaction (2) is second-order and the monomerization reaction is first-order, the corresponding equilibrium constant is given by eqn. (3), assuming activities are equal to concentrations. A

$$A^{\bullet -} + A^{\bullet -} \rightleftharpoons A_2^{2-} \quad (2)$$

$$K_{eq} = \frac{[A_2^{2-}]}{[A^{\bullet -}]^2} \quad (3)$$

simplified calculation shows that if the concentration of A_2^{2-} is *ca.* 0.5 mM, then the concentration of $A^{\bullet -}$ can be estimated to be *ca.* 0.2–0.07 mM (for $K_{eq} = 10^4$–10^5 L mol^{-1}), a range of concentrations of radical anions that are readily detectable under the experimental conditions used in this paper. It was observed that the signal intensities of the ester radical anions were *ca.* 1/10 to 1/3 the signal intensity of the stable anion radical of 7,7,8,8-tetracyanoquinodimethane ($TCNQ^{\bullet -}$) which was generated electrochemically under the same experimental conditions and initial concentration as the ester radical anions. Therefore, the relative EPR signal intensities are consistent with the K_{eq}-values given in Table 1.

An alternative explanation for the higher than expected stability of the (S) ester anion radicals was made on the basis that the detected radicals were reaction products of the primary radicals,[2] but this can now be discounted for the following reasons. First, the (O) ester radicals are known to undergo a very simple cleavage reaction in high yield (70–100%) by only one electron.[2] Considering the identity of the products and the number of electrons transferred, it is exceptionally difficult to propose a mechanism which accounts for a different moderately stable radical to be formed. Second, the EPR spectra are very simple, especially the benzene esters, and suggest a simple radical with high symmetry, making a dimer of more complicated reaction product radical very unlikely.

From the present experimental data, it is difficult to conclude whether the dimer dianion is intermolecularly π- or σ-bonded (or both as has been proposed for 9-substituted anthracenes[5a]). However, a σ-bonded dimer similar to the 2,6-diphenylphenolates[10] and *meta*-substituted dicyanobenzenes,[19] with the σ-bond formed between the aromatic rings in the *meta*-position to both carboxylate/carbothioate groups (*e.g.* **3**), is chemically feasible. One feature in the identification of the dimerization of 9-substituted anthracenes[4–7] and phenolates,[10] is that a dimer could be isolated as a stable product under bulk electrolysis conditions. While a simple σ-bonded dimer has not been isolated to date following reduction of the (O) and (S) diesters,[1–3] this is not surprising when it is considered that the radical ions are also decaying relatively quickly (see Scheme 1, step (5); and k_d in Table 1).

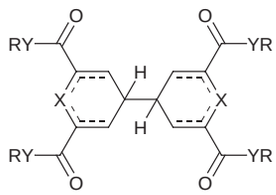

X = C or N, Y = O or S

3

It is significant to note that if the *para*-position to atom X (in **3**) is blocked, such as for dipropyl pyridine-3,5-dicarboxylate (**4**),[1] the electrochemistry and EPR spectroscopy changes substantially from what is observed for compounds **1a**–**2b**. Dipropyl pyridine-3,5-dicarboxylate shows completely chemically irreversible cyclic voltammetry up to the maximum scan rate examined of 50 V s^{-1}, and no EPR spectrum was observed under *in situ* electrolysis conditions in the very sensitive[27] channel electrode cell, indicating that any anion radicals that were formed were very unstable.

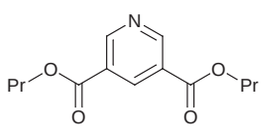

4

Conclusions

A combination of cyclic voltammetry and EPR spectroscopy experiments have shown that a likely explanation for the surprising stability of the anion radicals of dialkyl benzene-1,3-dicarboxylates, dialkyl pyridine-2,6-dicarboxylates and their corresponding dithioic *S*,*S*′-diesters is due to a reversible dimerization mechanism. The EPR data confirmed the existence of relatively stable anion radicals formed during the one electron reduction of the diesters, whose simple spectra suggested that the radicals responsible were the primary anions. The cyclic voltammetric data were complicated and digital simulation for an EC_{dim} mechanism required several homogeneous and heterogeneous rate constants in order to obtain a good theoretical match to the experimental data. Rate constants evaluated by simulation at scan rates between 0.1–50 V s^{-1} and substrate concentrations between 0.2–10 mM were estimated to be *ca.* 10^3–10^4 L mol^{-1} s^{-1} for the dimerization reaction and *ca.* 10^{-1}–10^0 s^{-1} for the monomerization reaction. The homogeneous reaction rates were consistent with signal intensity and stability data for the radical ions that were obtained by EPR spectroscopy, even considering the error associated with the voltammetric simulations from requiring a large number of variables.

Acknowledgements

RDW gratefully acknowledges La Trobe University, Department of Chemistry and Professor R. G. Compton, Oxford University, for the generous use of equipment. RDW also thanks the Ramsay Memorial Fellowships Trust for a Post-Doctoral Fellowship and Wadham College Oxford for a Lectureship.

References

1 R. D. Webster, A. M. Bond and R. G. Compton, *J. Phys. Chem.*, 1996, **100**, 10288.
2 (*a*) R. D. Webster, A. M. Bond and T. Schmidt, *J. Chem. Soc.*, *Perkin Trans. 2*, 1995, 1365; (*b*) R. D. Webster and A. M. Bond, *J. Org. Chem.*, 1997, **62**, 1779; (*c*) R. D. Webster and A. M. Bond, *J. Chem. Soc.*, *Perkin Trans. 2*, 1997, 1079.
3 R. D. Webster, A. M. Bond and D. C. Coomber, *J. Electroanal. Chem.*, 1998, **422**, 217.
4 (*a*) A. Yildiz and H. Baumgärtel, *Ber. Bunsenges. Phys. Chem.*, 1977, **81**, 1177; (*b*) M. A. Oturan and A. Yildiz, *J. Electroanal. Chem.*, 1984, **161**, 377.
5 (*a*) O. Hammerich and V. D. Parker, *Acta Chem. Scand.*, *Ser. B*, 1981, **35**, 341; (*b*) V. D. Parker, *Acta Chem. Scand.*, *Ser. B*, 1981, **35**, 349; (*c*) O. Hammerich and V. D. Parker, *Acta Chem. Scand.*, *Ser. B*, 1983, **37**, 379; (*d*) O. Hammerich and V. D. Parker, *Acta Chem. Scand.*, *Ser. B*, 1983, **37**, 851.
6 (*a*) C. Amatore, J. Pinson and J. M. Savéant, *J. Electroanal. Chem.*, 1982, **137**, 143; (*b*) C. Amatore, J. Pinson and J. M. Savéant, *J. Electroanal. Chem.*, 1982, **139**, 193; (*c*) C. Amatore, D. Garreau, M. Hammi, J. Pinson and J. M. Savéant, *J. Electroanal. Chem.*, 1984, **184**, 1.
7 (*a*) C. Z. Smith and J. H. P. Utley, *J. Chem. Res.* (*S*), 1982, 18; (*b*) A. S. Mendkovich, L. V. Michalchenko and V. P. Gultyai, *J. Electroanal. Chem.*, 1987, **224**, 273.
8 R. M. Crooks and A. J. Bard, *J. Electroanal. Chem.*, 1988, **240**, 253.
9 (*a*) A. B. Suttie, *Tetrahedron Lett.*, 1969, **12**, 953; (*b*) E. T. Denisov and I. V. Khudyakov, *Chem. Rev.*, 1987, **87**, 1313; (*c*) J. A. Richards, P. E. Whitson and D. H. Evans, *J. Electroanal. Chem.*, 1975, **63**, 311; (*d*) J. A. Richards and D. H. Evans, *J. Electroanal. Chem.*, 1977, **81**, 171.
10 (*a*) D. H. Evans, P. J. Jimenez and M. J. Kelly, *J. Electroanal. Chem.*, 1984, **163**, 145; (*b*) P. Hapiot and J. Pinson, *J. Electroanal. Chem.*, 1993, **362**, 257.
11 (*a*) A. Smie and J. Heinze, *Angew. Chem.*, *Int. Ed. Engl.*, 1997, **36**, 363; (*b*) P. Tschuncky, J. Heinze, A. Smie, G. Engelmann and G. Koßmehl, *J. Electroanal. Chem.*, 1997, **433**, 223; (*c*) J. Heinze, P. Tschuncky and A. Smie, *J. Solid State Electrochem.*, 1998, **2**, 102.
12 (*a*) P. Audebert and P. Hapiot, *Synthetic Metals*, 1995, **75**, 95; (*b*) P. Hapiot, L. Gaillon, P. Audebert, J. J. E. Moreau, J. P. LerePorte and M. W. C. Man, *J. Electroanal. Chem.*, 1997, **435**, 85.
13 S. Picart and E. Genies, *J. Electroanal. Chem.*, 1996, **408**, 53.
14 L. J. Kepley and A. J. Bard, *J. Electrochem. Soc.*, 1995, **142**, 4129.
15 V. D. Parker, *Acta Chem. Scand.*, 1998, **52**, 154.
16 (*a*) E. M. Kosower and J. L. Cotter, *J. Am. Chem. Soc.*, 1964, **86**, 5524; (*b*) M. J. Blandamer, M. F. Fox, M. C. R. Symons and G. S. P. Verma, *J. Chem. Soc.*, *Chem. Commun.*, 1966, 844; (*c*) M. J. Blandamer, J. A. Brivati, M. F. Fox, M. C. R. Symons and G. S. P. Verma, *Trans. Faraday Soc.*, 1967, **63**, 1850; (*d*) J. F. Stargardt and F. M. Hawkridge, *Anal. Chim. Acta*, 1983, **146**, 1; (*e*) M. Lapkowski and G. Bidan, *J. Electroanal. Chem.*, 1993, **362**, 249; (*f*) J. Mizuguchi and H. Karfunkel, *Ber. Bunsenges. Phys. Chem.*, 1993, **97**, 1466; (*g*) K. Komeers, *J. Chem. Res.* (*S*), 1994, 293; (*h*) R. D. Webster, R. A. W. Dryfe, J. C. Eklund, C.-W. Lee and R. G. Compton, *J. Electroanal. Chem.*, 1996, **402**, 167; (*i*) J. A. Alden, J. A. Cooper, F. Hutchinson, F. Prieto and R. G. Compton, *J. Electroanal. Chem.*, 1997, **432**, 63.
17 (*a*) B. M. Bezilla and J. T. Maloy, *J. Electrochem. Soc.*, 1979, **126**, 579; (*b*) R. D. Grypa and J. T. Maloy, *J. Electrochem. Soc.*, 1975, **122**, 509.
18 M. Svaan and V. D. Parker, *Acta Chem. Scand.*, 1985, **39**, 445.
19 M. Sertel, A. Yildiz, R. Gambert and H. Baumgärtel, *Electrochimica Acta*, 1986, **31**, 1287.
20 M. L. Andersen, M. F. Nielsen and O. Hammerich, *Acta Chem. Scand.*, 1997, **51**, 94.
21 D. H. Evans, S. E. Treimer and K. Hu, *J. Electroanal. Chem.*, 1997, **438**, 173.
22 S. A. Lerke, D. H. Evans and P. J. Fagan, *J. Electrochem. Soc.*, 1997, **144**, 4223.
23 M. M. Bates, T. J. Cardwell, R. W. Cattrall, L. W. Deady and C. G. Gregorio, *Talanta*, 1995, **42**, 999.
24 (*a*) T. Osa and T. Kuwana, *J. Electroanal. Chem.*, 1969, **22**, 389; (*b*) A. J. Fry and W. E. Britton, in *Laboratory Techniques in Electroanalytical Chemistry*, ed. P. T. Kissinger and W. R. Heineman, Marcel Dekker, New York, 1984, ch. 13.
25 (*a*) Digisim by Bioanalytical Systems Inc. (BAS), 2701 Kent Avenue, West Lafayette IN 47906, USA; (*b*) M. Rudolph, D. P. Reddy and S. W. Felberg, *Anal. Chem.*, 1994, **66**, 589A.
26 C. Nervi, *Electrochemical Simulations Package*, Version 2.4, http://chpc06.ch.unito.it/esp_manual.html.
27 (*a*) B. A. Coles and R. G. Compton, *J. Electroanal. Chem.*, 1983, **144**, 87; (*b*) R. G. Compton and A. M. Waller, in *Spectroelectrochemistry: Theory and Practice*, ed. R. J. Gale, Plenum Press, New York, 1988, ch. 7; (*c*) R. D. Webster, A. M. Bond, B. A. Coles and R. G. Compton, *J. Electroanal. Chem.*, 1996, **404**, 303.
28 (*a*) R. S. Nicholson and I. Shain, *Anal. Chem.*, 1964, **36**, 706; (*b*) R. S. Nicholson, *Anal. Chem.* 1966, **38**, 1406.
29 J. H. Wagenknecht, R. D. Goodin, P. J. Kinlen and F. E. Woodard, *J. Electrochem. Soc.*, 1984, **131**, 1559.
30 C. R. Wilke and P. Chang, *AIChE J.*, 1955, **1**, 264.
31 R. L. Wang, K. Y. Tam and R. G. Compton, *J. Electroanal. Chem.*, 1997, **434**, 105.
32 R. J. Gale ed., in *Spectroelectrochemistry: Theory and Practice*, Plenum Press, New York, 1988.
33 M. Hirayama, *Bull. Chem. Soc. Jpn.*, 1967, **40**, 2234.
34 J. Voss, W. Schmüser and K. Schlapkohl, *J. Chem. Res.* (*S*), 1977, 144.

Paper 8/06854B